Surface Alfven Wave Reflection as the Slow Wind Formation Mechanism in the Alfven Wave Driven Solar Atmosphere Model

.

Igor V. Sokolov[1], Bart van der Holst[1] , Ch. Nick Arge[2], Lulu Zhao[1], and Tamas Gombosi[1]

1. **[1]CLaSP, University of Michigan, Ann Arbor MI**
2. **[2]Goddard Space Flight Center, Greenbelt MD**

3. SH032-07
4. December, 11 2020 (10:54 - 10:58 PST)

Computational Models for Solar Wind

- Solar wind is the plasma state at 15-30 R_S, <R < 1AU.
- Features:
  - Windy (outward motional speed dominates over all other characteristic speed: thermal, Alfven ets)
  - Bimodal structure: fast (and rarefied, and electrons stay cold on the way – low charge states of oxygen) wind and slow (and intermittent, and dense, and electrons are hot somewhere on the way: higher charge states of oxygen)
- WSA semi-empirical model is a gold standard to predict the solar wind speed

AWSoM Model

- The Alfven Wave turbulence based Solar atmosphere Model (AWSoM) employs the turbulent dissipation as the unified mechanism to explain both the coronal heating in the closed field region and powering and accelerating the solar wind.
- The pronounced difference in the heating efficiency between the closed field region and coronal holes is attributed to the physical properties of Alfven wave turbulence, namely, that the nonlinear dissipation of the Alfven wave of the given direction is proportional to an amplitude of the oppositely propagating wave.

SWMF/AWSoM Model

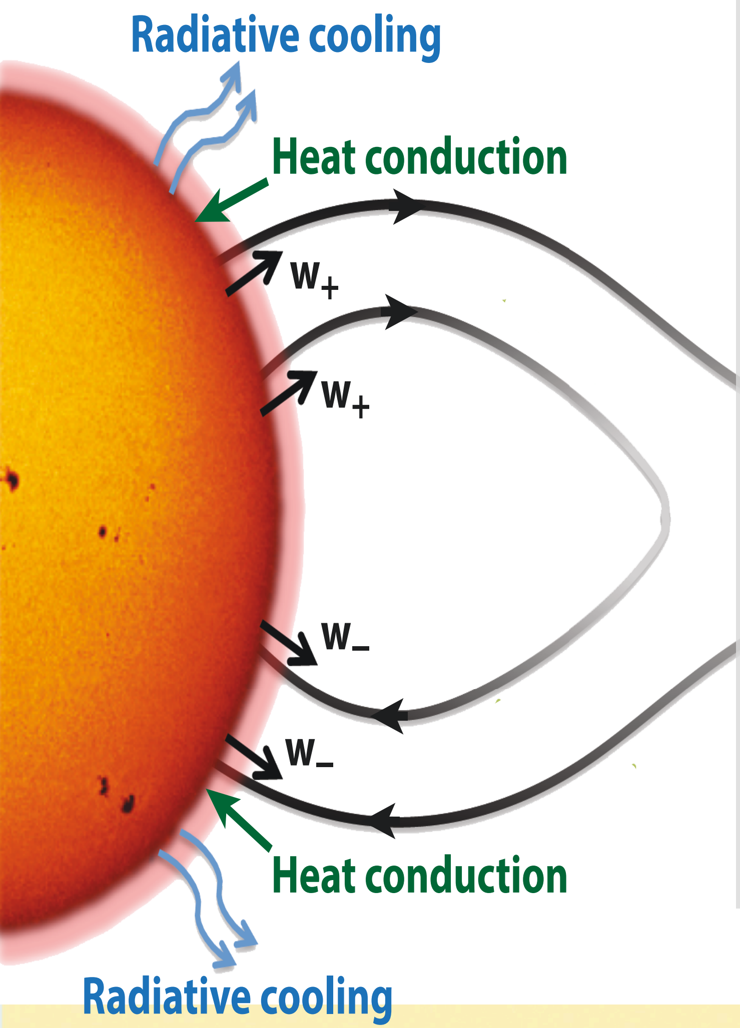

Heat conduction: Spitzer ($r<5R_s$) + Hollweg ($r>5R_s$)
Radiative cooling from CHIANTI
Wave pressure gradient accelerates and heats
Two (T_i, T_e) or three ($T_{i\parallel}$, $T_{i\perp}$, T_e) temperatures
Turbulent energy transport along field lines:

$$\frac{\partial w_\pm}{\partial t} + \nabla\cdot\left[\left(\mathbf{u}\pm\mathbf{V}_A\right) w_\pm\right] + \frac{w_\pm}{2}\left(\nabla\cdot\mathbf{u}\right) = \mp\mathcal{R}\sqrt{w_- w_+} - \Gamma_\pm w_\pm$$

$$\Gamma_\pm = \frac{2}{L_\perp}\sqrt{\frac{w_\mp}{\rho}} \qquad L_\perp\sqrt{B} = 150\ \mathrm{km}\sqrt{T} \qquad (\square / B) = 1.1\times 10^6\ \mathrm{W m^{-2} T^{-1}}$$

$$\mathcal{R} = \min\{\mathcal{R}_{imb}, \max\left[\Gamma_\pm\right]\}\begin{cases}\left(1-2\sqrt{\frac{w_-}{w_+}}\right) & w_+ \geq 4w_- \\ 0 & \frac{1}{4}w_- < w_+ < 4w_- \\ \left(2\sqrt{\frac{w_-}{w_+}}-1\right) & w_+ \leq \frac{1}{4}w_-\end{cases}$$

$$\mathcal{R}_{imb} = \sqrt{\left[\left(\mathbf{V}_A\cdot\nabla\right)\log V_A\right]^2 + \left[\frac{\mathbf{B}}{B}\cdot\left(\nabla\times\mathbf{u}\right)\right]^2}$$

Sokolov et al., ApJ, **764**, 23 (2013).
van der Holst et al., ApJ, **782**, 81 (2014).

Wave Reflection in the AWSoM Model

- Thus, in the closed field region the efficient heating occurs, since the waves propagating from two ends of the closed line form a balanced turbulence with a high dissipation efficiency.
- To the contrary, within coronal holes the field lines are open, so that the outward propagating waves dominate. The only source for the inward propagating wave is the comparatively weak reflection of the dominant waves, resulting in gradually heating the solar wind as well its acceleration by the turbulent pressure.

Alfvén Wave Reflection

- **Wave energy densities of counter-propagating transverse Alfvén waves parallel (+) and anti-parallel (-) to magnetic field:**

$$\frac{\partial w_\pm}{\partial t} + \nabla\cdot\Big[\underbrace{(\mathbf{u} \pm \mathbf{V}_A)}_{\text{Alfvén wave advection}} w_\pm\Big] + \overbrace{\frac{w_\pm}{2}(\nabla\cdot\mathbf{u})}^{\text{energy reduction in expanding flow}} = \underbrace{\mp\mathcal{R}\sqrt{w_- w_+}}_{\text{wave reflection}} \overbrace{- \Gamma_\pm w_\pm}^{\text{wave dissipation}}$$

$$\mathcal{R} = \min\Big[\sqrt{[(\mathbf{V}_A\cdot\nabla)\log V_A]^2 + (\mathbf{b}\cdot[\nabla\times\mathbf{u}])^2}, \max(\Gamma_\pm)\Big] \begin{cases} \left(1 - 2\sqrt{\dfrac{w_-}{w_+}}\right) & \text{if} \quad 4w_- \le w_+ \\ 0 & \text{if} \quad \tfrac{1}{4}w_- \le w_+ \le 4w_- \\ \left(2\sqrt{\dfrac{w_+}{w_-}} - 1\right) & \text{if} \quad 4w_+ \le w_- \end{cases}$$

Slow Wind Originates in the Close Proximity of the Coronal Hole Boundary

- This unified model explains the EUV images with a contrast between hot and dense (hence, bright) closed field region, and cooler rarefied (hence, dark) coronal hole plasma. However, the description of the slow solar wind speed is not perfect and worse than that provided by the WSA model.
- Here, we incorporate one of the WSA model features, namely, the dependence of the solar wind speed on the angular distance from the coronal hole boundary to the footprint of the magnetic field line connecting the observation point to the Sun. The closer is the coronal hole boundary, the slower is the solar wind:

```
VELEQN  = 285 + 625/((1 + fexp)**0.22222) * (1.0 - 0.8* &
exp(-(arc_ft_bd/2)**2) )**3
```

- The present shortcoming of the AWSoM solar wind is that the closed field region proximity is not accounted for.

Account for the Proximity of the Coronal Hole Boundary in the AWSoM

- We start from equation for the Elsasser variables $\mathbf{z}_\pm = \delta\mathbf{u} \mp \delta\mathbf{B}/\sqrt{\mu_0\rho}$ in van der Holst et al., ApJ, 782, 81 (2014), which relate the Alfven wave oscillations of the velocity and magnetic field in the directions, perpendicular to the regular magnetic field:

$$\frac{d_\pm \mathbf{z}_\pm}{dt} + \mathbf{z}_\mp \cdot \nabla \mathbf{u} \mp \frac{\mathbf{z}_\mp \cdot \nabla \mathbf{B}}{\sqrt{\mu_0\rho}} - \frac{\mathbf{z}_\pm - \mathbf{z}_\mp}{4\rho}\frac{d_\mp \rho}{dt} = 0,$$

where $\frac{d_\pm}{dt} = \frac{\partial}{\partial t} + (\mathbf{u} \pm \mathbf{V}_A + \mathbf{z}_\mp)\cdot\nabla$ and $\mathbf{V}_A = \frac{\mathbf{B}}{\sqrt{\mu_0\rho}}$.

- Equations for the wave energy densities, $w_\pm = \rho \mathbf{z}_\pm^2/4$, thus read:

$$\frac{\partial w_\pm}{\partial t} + \nabla\cdot[(\mathbf{u} \pm \mathbf{V}_A + \mathbf{z}_\mp) w_\pm] + \frac{w_\pm}{2}(\nabla\cdot\mathbf{u}) + \frac{\rho}{2}\mathbf{z}_\pm \cdot [(\mathbf{z}_\mp\cdot\nabla)\mathbf{u} \mp \frac{(\mathbf{z}_\mp\cdot\nabla)\mathbf{B}}{\sqrt{\mu_0\rho}}] + \frac{\mathbf{z}_+\cdot\mathbf{z}_-}{8}\frac{d_\mp\rho}{dt} = 0.$$

- The only distinction from van der Holst et al., ApJ, 782, 81 (2014) is that in the equation for density derivative (the last term in LHS):

$$\frac{1}{\rho}\frac{d_\mp \rho}{dt} = -\nabla\cdot\mathbf{u} \mp \mathbf{V}_A\cdot\nabla\log\rho + \frac{\mathbf{z}_\pm - \mathbf{z}_\mp}{2}\cdot\nabla\log\rho$$

we account for the last non-linear term with density gradient.

An Extra Non-linear Wave Reflection Occurs Near the Coronal Hole Boundary

- Why non-linear? Because it depends on the wave amplitude:
- Why reflection (rather than quite similar non-linear dissipation)? Because (see plus/minus signs) it attenuates the dominant wave and amplifies the minor wave, however, does not change the total wave energy density (as the dissipation would do).
- Why does it occur near the boundary between the coronal hole and closed field region? Because the difference in the plasma density between these regions (due to the said distinction in heating mechanisms) results in high density gradient in the direction perpendicular to the magnetic field.

$$\mathcal{R}_{\rm imb} = \sqrt{(\mathbf{b}\cdot[\nabla\times\mathbf{u}])^2 + [(\mathbf{V}_A\cdot\nabla)\log V_A]^2 + \frac{\max(w_\pm)}{\rho}\left[\nabla_\perp \log\sqrt{\rho}\right]^2}.$$

- This result is well compatible with the WSA model assumptions.
- It is well compatible with the remote observations: high density gradients and high temperature near the coronal hole boundary.

Reproduction of the solar wind observations at 1 AU

Without extra reflection

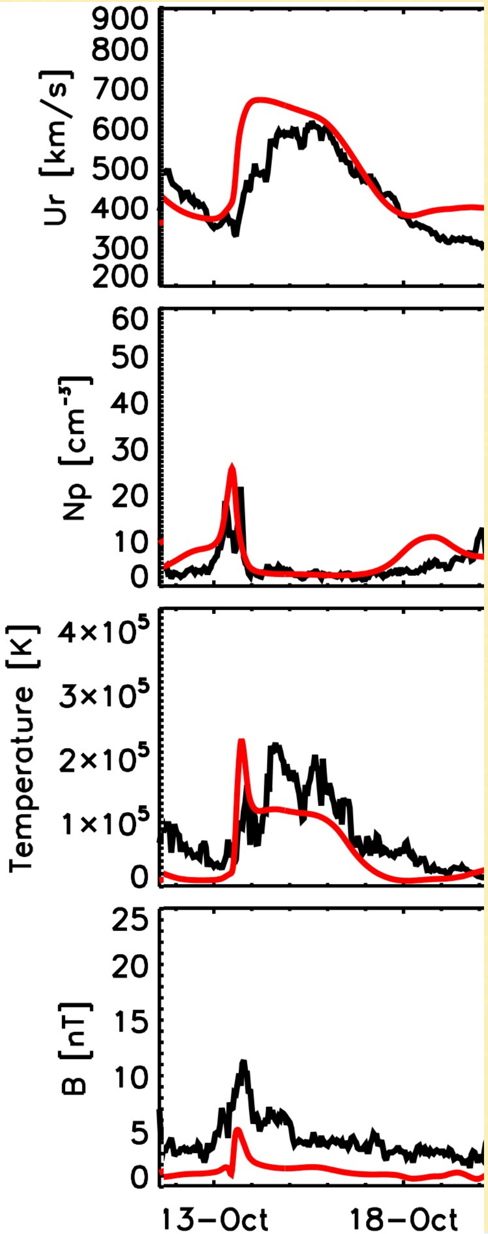

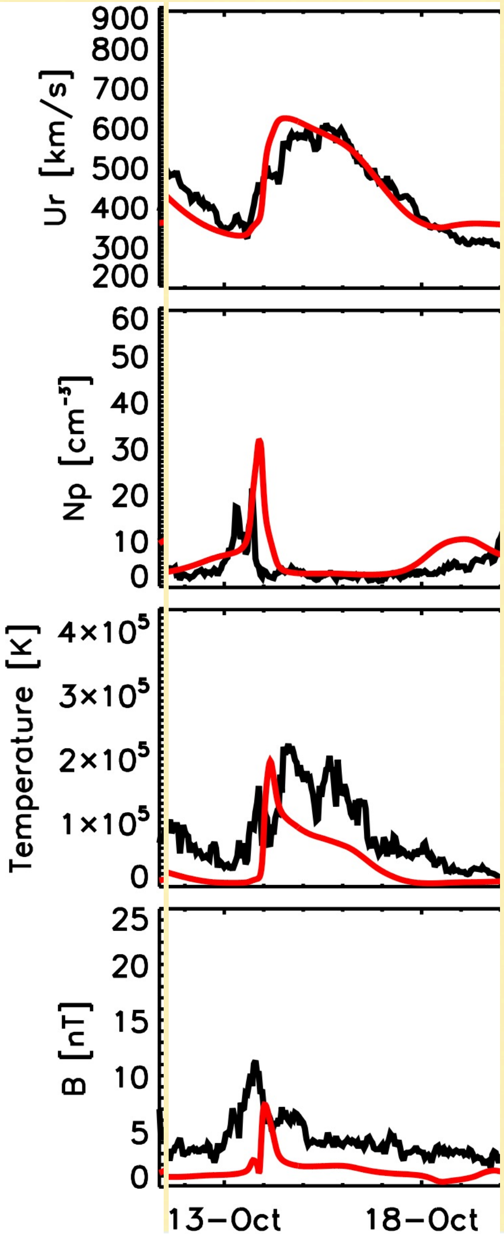

With extra reflection

Gong-ADAPT Magnetogram 2018-10-13 T06:00:00

Conclusion

- The heating near the coronal hole boundary is included into the AWSoM model via the Alfven wave interaction with the boundary between the closed and open field lines.
- Although the excessive heating on the Alfven surface wave is possible (Evans et al 2012), we chose to parameterize the surface effect in terms of excessive nonlinear reflection proportional to the transverse gradient of density.
- The efficiency of such reflection is derived analytically and compared with the solar wind observation data at 1 AU.

Future Work

- We will add a new capability to the existing automated real-time simulation system. By comparing the AWSoM predictions with the WSA predictions at 0.1 AU, we will be able to adjust the model parameters separately for the fast and slow solar wind.

Acknowledgement

- We acknowledge the support from the NASA LWS grant 80NSSC17K0686 as well as from NSF1836821 grant by the Space Weather Operations-to-Research (O2R) program.